1

Solar Cell

Purnomo Sidi Priambodo, Nji Raden Poespawati and Djoko Hartanto
Universitas Indonesia
Indonesia

1. Introduction

Solar cell is the most potential energy source for the future, due to its characteristics of renewable and pollution free. However, the recent technology still does not achieve high Watt/m^2 and cost efficiency. Solar cell technology still needs to be developed and improved further to obtain optimal efficiency and cost. Moreover, in order to analyze and develop the solar cell technologies, it is required the understanding of solar cell fundamental concepts. The fundamentals how the solar works include 2 phenomena, i.e.: (1) Photonics electron excitation effect to generate electron-hole pairs in materials and (2) diode rectifying.

The phenomenon of photonics electron excitation is general nature evidence in any materials which absorbs photonic energy, where the photonic wavelength corresponds to energy that sufficient to excite the external orbit electrons in the bulk material. The excitation process generates electron-hole pairs which each own quantum momentum corresponds to the absorbed energy. Naturally, the separated electron and hole will be recombined with other electron-holes in the bulk material. When the recombination is occurred, it means there is no conversion energy from photonics energy to electrical energy, because there is no external electrical load can utilize this natural recombination energy.

To utilize the energy conversion from photonic to electric, the energy conversion process should not be conducted in a bulk material, however, it must be conducted in a device which has rectifying function. The device with rectifying function in electronics is called diode. Inside diode device, which is illuminated and excited by incoming light, the electron-hole pairs are generated in *p* and *n*-parts of the *p*-*n* diode. The generated pairs are not instantly recombined in the surrounding exciting local area. However, due to rectifying function, holes will flow through *p*-part to the external electrical load, while the excited electron will flow through *n*-part to the external electrical load. Recombination process of generated electron-hole pairs ideally occurs after the generated electrons-holes experience energy degradation after passing through the external load outside of the diode device, such as shown in illustration on Figure-1.

The conventional structure of p-n diode is made by crystalline semiconductor materials of Group IV consists of silicon (Si) and germanium (Ge). As an illustration in this discussion, Si diode is used, as shown in Figure-1 above, the sun light impinges on the Si p-n diode, wavelengths shorter than the wavelength of Si bandgap energy, will be absorbed by the Si material of the diode, and exciting the external orbit electrons of the Si atoms. The electron excitation process causes the generation of electron-hole pair. The wavelengths longer than the wavelength of Si bandgap energy, will not be absorbed and not cause excitation process

to generate electron-hole pair. The excitation and electron-hole pair generation processes are engineered such that to be a useful photon to electric conversion. The fact that electron excitation occurs on $\lambda < \lambda_{bandgap\text{-}Si}$, shows the maximum limit possibility of energy conversion from sun-light to electricity, for solar cell made based on Si.

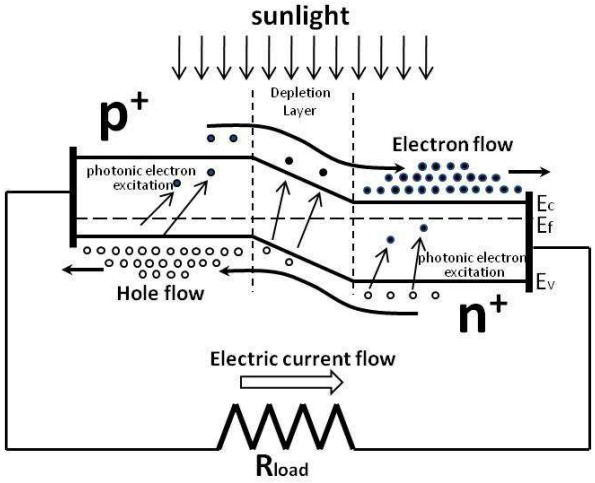

Fig. 1. Illustration of solar cell device structure in the form of p-n diode with external load. The holes flow to the left through the valanche band of diode p-part and the electrons flow through the conduction band of diode n-part.

The fundamental structure of solar cell diode does not change. The researchers have made abundance engineering experiment to improve efficiency by involving many different materials and alloys and also restructuring the solar cell fundamental structure for the following reasons:

1. Energy conversion efficiency Watt/m2 improvement from photon to electricity.
2. Utilization of lower cost material that large availability in nature
3. Utilization of recyclable materials
4. The simplification of fabrication process and less waste materials
5. Longer solar cell life time

In this Chapter, we will discuss several topics, such as: (1) Solar cell device in an ideal diode perspective; (2) Engineering methods to improve conversion energy efficiency per unit area by involving device-structure engineering and material alloys; (3) Standar solar cell fabrications and (4) Dye-sensitized solar cell (DSSC) as an alternative for inexpenssive technology.

2. Solar cell device in an ideal diode perspective

In order to be able to analyze further the solar cell performance, we need to understand the concepts of an ideal diode, as discussed in the following explanation. In general, an ideal diode with no illumination of light, will have a dark *I-V* equation as following [1]:

$$I = I_0\left(e^{qV/k_BT} - 1\right) \tag{1}$$

where I is current through the diode at forward or reverse bias condition. While, I_0 is a well known diode saturation current at reverse bias condition. T is an absolute temperature ^oK, k_B is Boltzmann constant, q (> 0) is an electron charge and V is the voltage between two terminals of p-n ideal diode. The current capacity of the diode can be controlled by designing the diode saturation current I_0 parameter, which is governed by the following equation [1]:

$$I_0 = qA\left(\frac{D_e}{L_e}\frac{n_i^2}{N_A} + \frac{D_h}{L_h}\frac{n_i^2}{N_D}\right) \tag{2}$$

where A is cross-section area of the diode, n_i is concentration or number of intrinsic electron-hole pair /cm^3, D_e is the diffusion coefficient of negative (electron) charge, D_h is the diffusion coefficient of positive (hole) charge, L_e and L_h are minority carrier diffusion lengths, N_A is the extrinsic acceptor concentration at p-diode side and N_D is the extrinsic donor concentration at n-diode side [1].

$$L_e = \sqrt{D_e\tau_e} \text{ dan } L_h = \sqrt{D_h\tau_h} \tag{3}$$

where τ_e and τ_h are minority carrier lifetime constants, which depend on the material types used. From Equations (2) & (3) above, it is clearly shown that the diode saturation current I_0 is very depended on the structure and materials of the diode. The I-V relationship of a dark condition is shown on Figure-2.

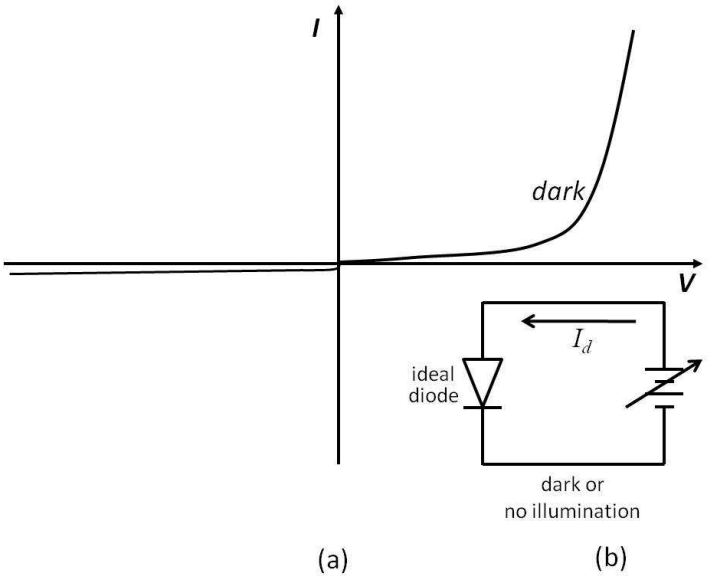

Fig. 2. I-V relationship of ideal diode for dark or no illumination. (a) I-V graph and (b) the equivalent ideal diode circuit.

Furthermore, if an ideal diode is designed as a solar cell, when illuminated by sun-light, there will be an energy conversion from photon to electricity as illustrated by a circuit model shown on Figure-3. As already explained on Figure-1 that the electron excitation caused by photon energy from the sun, will corresponds to generation of electron-hole pair, which electron and hole are flowing through their own bands. The excited electron flow will be recombined with the hole flow after the energy reduced due to absortion by the external load.

The circuit model of Figure-3, shows a condition when an ideal diode illuminated, the ideal diode becomes a current source with an external load having a voltage drop ***V***. The total output current, which is a form of energy conversion from illumination photon to electricity, is represented in the form of superposition of currents, which are resulted due to photon illumination and forward current bias caused by positive voltage across *p* and *n* terminals. The corresponding *I-V* characteristic of an ideal diode solar cell is described by the Shockley solar cell equation as follows [3]:

$$I = I_{photon} - I_0\left(e^{qV/k_BT} - 1\right) \tag{4}$$

I_{photon} is the photogenerated current, closely related to the photon flux incident to the solar cell. In general, I_{photon} can be written in the following formula [2]

$$I_{photon} = qAG\left(L_e + W + L_h\right) \tag{5}$$

where *G* is the electron-hole pair generation rate of the diode, *W* is depletion region width of the solar cell diode. The *G* value absolutely depends on material types used for the device and the illumination spectrum and intensity (see Eq 14a & b), while *W* value depends on the device structure, A is the cross-section of illuminated area. The *I-V* characteristic of an ideal diode solar cell is illustrated in Figure-4.

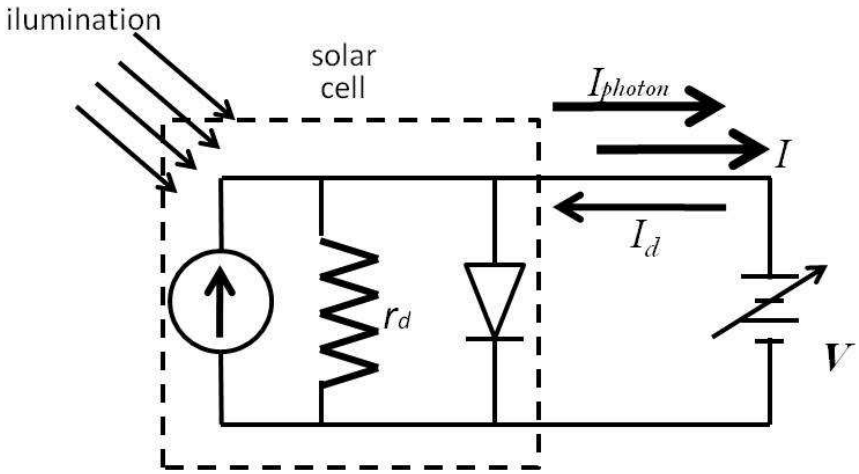

Fig. 3. The equivalent circuit model of an ideal diode solar cell.

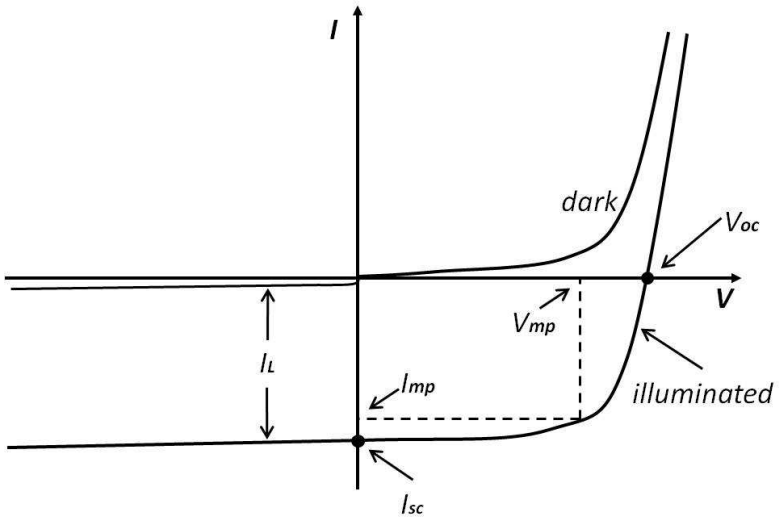

Fig. 4. The Graph of the I-V characteristics of an ideal diode solar cell when non-illuminated (dark) and illuminated.

Solar cell output parameters

From Figure-4, it is shown that there are 4 output parameters, which have to be considered in solar cell. The first parameter is I_{SC} that is short circuit current output of solar cell, which is measured when the output terminal is shorted or V is equal to 0. The value of output current $I = I_{SC} = I_{photon}$ represents the current delivery capacity of solar cell at a certain illumination level and is represented by Equation (4). The second parameter is V_{OC} that is the open circuit output voltage of solar cell, which is measured when the output terminal is opened or I is equal to 0. The value of output voltage V_{OC} represents the maximum output voltage of solar cell at a certain illumination level and can be derived from Equation (4) with output current value setting at $I = 0$, as follows:

$$V_{OC} = \frac{k_B T}{q} \ln\left(\frac{I_{photon}}{I_0} + 1\right) \tag{6}$$

In general, V_{OC} is determined by I_{photon}, I_0 and temperature, where I_0 absolutely depends on the structure design and the choice of materials for solar cell diode, while I_{photon} besides depending on the structure design and the choice of materials, depends on the illumination intensity as well.

The maximum delivery output power is represented by the area of product V_{MP} by I_{MP} as the maximum possible area at fourth quadrant of Figure-4.

$$P_{MP} = V_{MP} \cdot I_{MP} \tag{7}$$

The third parameter is fill factor *FF* that represents the ratio PMP to the product V_{OC} and I_{SC}. This parameter gives an insight about how "square" is the output characteristic.

$$FF = \frac{P_{MP}}{V_{OC} \cdot I_{SC}} = \frac{V_{MP} \cdot I_{MP}}{V_{OC} \cdot I_{SC}} \tag{8}$$

In the case of solar cell with sufficient efficiency, in general, it has FF between 0.7 and 0.85. The energy –conversion efficiency, η as the fourth parameter can be written as [2]

$$\eta = \frac{V_{MP} \cdot I_{MP}}{P_{in}} = \frac{V_{OC} \cdot I_{SC} \cdot FF}{P_{in}} \tag{9}$$

where P_{in} is the total power of light illumination on the cell. Energy-conversion efficiency of commercial solar cells typically lies between 12 and 14 % [2]. In designing a good solar cell, we have to consider and put any effort to make those four parameters I_{SC} , V_{OC} , FF and η as optimum as possible. We like to use term optimum than maximum, since the effort to obtain one parameter maximum in designing solar cell, will degrade other parameters. Hence the best is considering the optimum efficiency of solar cell.

3. Improvement of solar cell performance

In the process to improve solar cell output performance that is energy conversion efficiency from photon to electricity, which is typically lies between 12 to 14 % [2], the researchers have been conducting many efforts which can be categorized and focused on:

1. Diode device structure engineering to improve current output I_{sc}, by reducing I_0 and increasing photon illumination conversion to I_{photon} in the form of improving G parameter, electron-hole pair generation constant. The diode structure engineering, at the same time also improving output voltage in the form of V_{OC}, and improving FF and finally improving the energy conversion efficiency from photon to electricity.
2. Material engineering, especially to obtain improvement on G parameter, electron-hole pair generation.
3. Device structure engineering to improve quantum efficiency and lowering top-surface lateral current flow to reduce internal resistance.
4. Solar cell structure engineering includes concentrating photon energy to the solar cell device.

3.1 Solar cell diode structure engineering

In general, sun-light illuminates solar cell with the direction as shown on Figure-5.

The light illumination with $\lambda > \lambda_{bandgap}$ will pass through without absorbed by solar cell. While the light with $\lambda < \lambda_{bandgap}$ will be absorbed. Whatever spectrum, basically, incident light with $\lambda < \lambda_{bandgap}$ will be absorbed as a function of exponential decay with respect to distance parameter as $e^{-\alpha(\lambda)z}$ from the top surface, where $a(\lambda)$ is absorption coefficient and z is the depth distance in the solar cell diode. Absorption occurs at any absorbed wavelength are shown on Figure-6.

As shown on Figure-6, red light will be absorbed exponentially slower than the blue light. The photons with different wavelengths will be absorbed in different speed. This discrepancy can be explained and derived by using the probability of state occupancies in material, which is illustrated by Fermi function as follows [1]:

$$f(E) = \frac{1}{\exp\left[\left(E - E_f\right) / k_B T\right] + 1} \tag{10}$$

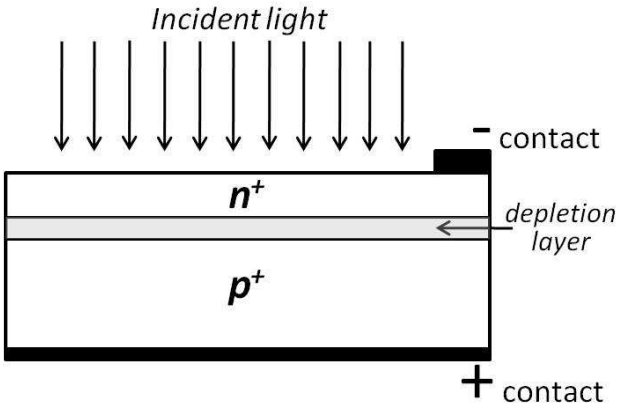

Fig. 5. A generic solar cell diode structure and the incidence light direction

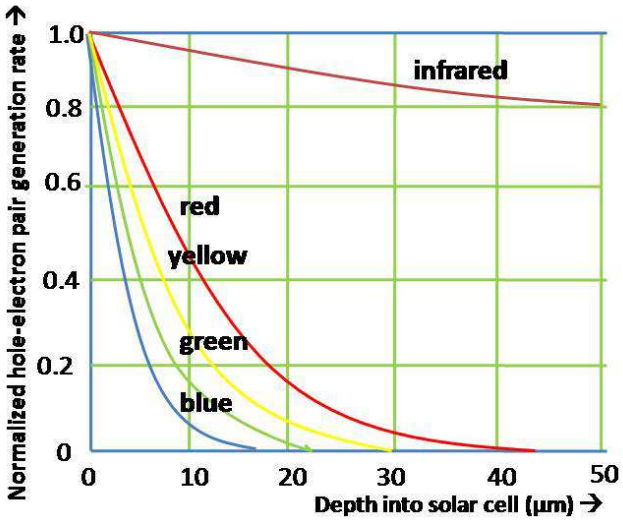

Fig. 6. A normalized hole-electron pair generation rate [2].

when $\exp\left[\left(E-E_f\right)/k_BT\right] >> 1$, then Equation (10) can be written as

$$f(E) \approx e^{-\left[\left(E-E_f\right)/k_BT\right]} \tag{11}$$

where E represents the energy state in crystalline. Moreover, photon absorption $a(\lambda)$ by material is an equal representation of excitation probability of electron leaving hole towards a state in conduction band after excited by a photon. The probability is the integral accumulation of multiplication between electron occupation probability in valence band

and probability of possible state that can be occupied by the excited electron, furthermore those two are multiplied by a coefficient $\sigma(\lambda)$ as shown in the following equation:

$$\alpha(\lambda) \approx \sigma(\lambda) \cdot \int_{E_c - \frac{hc}{\lambda}}^{E_v} f(E) \cdot (1 - f(E + \frac{hc}{\lambda})) \cdot dE \tag{12}$$

where $\sigma(\lambda)$ is a cross section probability parameter represent of possible occurrence the photon to hole-electron pair generation at wavelength λ. Parameter $\sigma(\lambda)$ is obtained by the following derivation [2]:

$$\sigma(\lambda) = D\left(\frac{\left(hc/\lambda - E_g + E_p\right)^2}{\exp(E_p / k_B T) - 1} + \frac{\left(hc/\lambda - E_g - E_p\right)^2}{1 - \exp(E_p / k_B T)} \right) \tag{13}$$

where parameters D, Eg and Ep depend on material types used and crystalline quality, and usually are obtained by conducting experiments. Eg and Ep each are bandgap energy dan phonon absorption or emission energy respectively, h is the Plank constant and c is the light speed in vacuum. The $\sigma(\lambda)$ parameter is a function of λ and naturally depends on the type of the material. Parameter absorption $a(\lambda)$ on Equation (12) when multiplied by illumination intensity $I_{int}(\lambda)$, will represent the generation rate of hole-electron pairs at λ or $G(\lambda)$.

$$G(\lambda) = \alpha(\lambda) \cdot I_{\text{int}}(\lambda) \approx \sigma(\lambda) \cdot I_{\text{int}}(\lambda) \int_{E_c - \frac{hc}{\lambda}}^{E_v} f(E) \cdot (1 - f(E + \frac{hc}{\lambda})) \cdot dE \tag{14-a}$$

Furthermore, the generation rate of hole-electron pair G can be written as the integral of $G(\lambda)$ as following:

$$G = \int_0^{\lambda_{bandgap}} G(\lambda)\, d\lambda \tag{14-b}$$

In a glance, the terms multiplication under the integral and the integral limits of Equations (12 and 14a) show that parameter values $G(\lambda)$ or $a(\lambda)$ getting larger for λ becoming shorter (agrees to Figure-6). $\lambda_{bandgap}$ is the λ of the bandgap energy as the limit of irradiance photon to electric conversion. At $\lambda > \lambda_{\text{bandgap}}$, $\sigma(\lambda)$ is zero and will not be absorbed or there is no electron-hole generation and does not contribute to the conversion. The following Figure-7 illustrates the distribution state of a material with respect to the Fermi function. The transition state probability represents the photon to hole-electron pair generation.

Back to Figure-5, naturally layer n^+ is a layer that more easier to generate hole-electron pairs due to photon excitation, in comparison to layer p^+. Hence, the n^+ layer is called as an electron emitter layer. By considering Figure-5 and 6 that photon absorption and hole-electron generation occurs at the front layer of diode structure, then in order to obtain higher conversion efficiency, the n^+ layer as electron emitter layer is located on the top surface of solar cell diode structure such as shown on Figure-5 above.

However, in order to be an effective electron emitter layer, the thickness of the n^+ layer must be shorter than the minority carrier diffusion length L_h in n^+ layer, where the hole minority

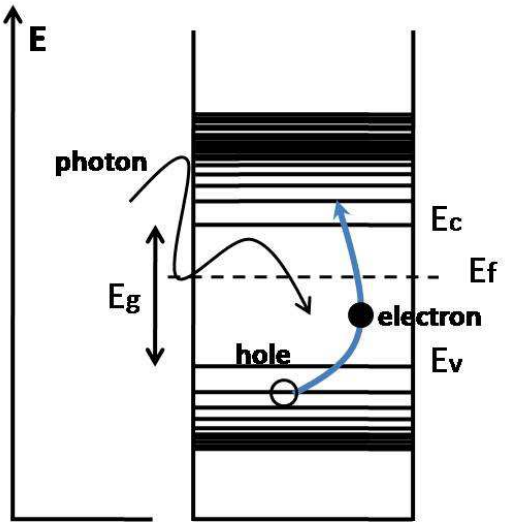

Fig. 7. Transition state probability illustration [4].

carrier diffusion lengths L_h is governed by Equation (3). If the thickness of n^+ layer > L_h, then most of hole-electron pairs experience local recombination, which means useless for photon to electrical energy conversion. Between n^+ and p^+ layers, there exists a depletion layer, which has a built in potential V_{bi} to conduct collection probability of the generated hole-electron pairs. The width of depletion layer can be written as follows [1]:

$$W = \left[\frac{2\varepsilon_r \varepsilon_0}{q} \left(\frac{N_A + N_D}{N_A \cdot N_D} \right) (V_{bi} - V_A) \right]^{1/2} \tag{15}$$

where W is the depletion layer width, V_{bi} is the diode built in potential and V_A is the applied or solar cell output voltage. The diode built in potential can be approach by the following Equation [1]:

$$V_{bi} = \frac{k_B T}{q} \ln \left(\frac{N_A N_D}{{n_i}^2} \right) \tag{16}$$

The collection probability describes the probability that the light absorbed in a certain region of the device will generate hole-electron pairs which will be collected by depletion layer at *p-n* junction. The collected charges contribute to the output current I_{photon}. However, the probability depends on the distance to the junction compared to the diffusion length. If the distance is longer than the diffusion length, then instead of contributing to the output current, those hole-electron pairs are locally recombined again, hence the collection probability is very low. The collection probability is normally high (normalized to 1) at the depletion layer. The following Figure-8 shows the occurrence of photon absorption by the device that illustrated as an exponential decay, at the same time, representing generation of hole-electron pairs. The collection probability shows that at the front (top) surface is low

because far from the built-in voltage at depletion layer. On depletion layer, collection probability very high and give a large contribution on output current I_{photon}.

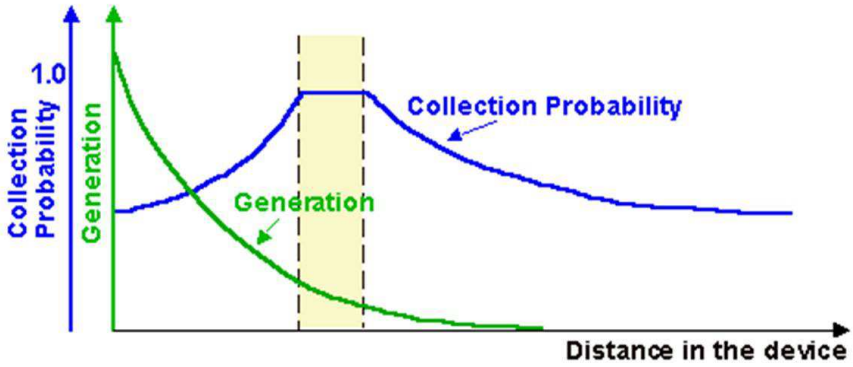

Fig. 8. The collection probability of the generated hole-electron pairs at junction [5].

As explained previously, there are 4 reference parameters in designing solar cell, i.e.: I_{sc}, V_{OC}, FF and η. By considering the equations of those 4 parameters, it is likely that the four parameters are correlated each other. For instance, in order to increase I_{sc} or I_{photon} (1st parameter), we have to consider Equation (5), where the structure will depend on 2 parameters i.e. A the area of the cell surface and W the thickness of the depletion layer. While parameters G, L_e and L_h depend on the materials used for the solar cell diode. Increasing A parameter (the area of diode) will not have impact to other parameters, however, increasing W parameter will have impact to other parameters. Of course, by increasing A, the total output current $I_{photonic}$ will increase proportionally, the increasing W, the length of collection probability of depletion layer will increase as well, where finally it is expected to improve contribution to the output current.

From Equations [15] dan [16], it is shown that structurally W parameter depends on N_A and N_D. In order to increase W proportionally linear, then what we can do is by reducing doping concentration of N_A and N_D or one of both. The consequence of reducing N_A and/or N_D is the linear increment of I_0, which in the end causing reducing the total output current such as shown in Equation (4). Don't be panic, improvement I_{SC} in one side and decreasing in other side due to concentration adjustment of N_A and/or N_D does not mean there is no meaning at all. Because at a certain N_A and/or N_D value $+\Delta I_{SC}$ that caused by ΔW can be much larger than $-\Delta I_{SC}$ that caused by I_0. Hence, to obtain the optimal design, it is required to apply a comprehensive numerical calculation and analysis to obtain the optimal I_{SC}.

For the sake of obtaining an optimal output voltage V_{OC} (2nd parameter), we have to consider Equation (6). The equation shows that V_{OC} is a natural logarithmic function of I_{SC}/I_0, it shows that by reducing N_A and/or N_D will cause on increasing I_{SC} in root square manner and linearly proportional to I_0 that causes decreasing of V_{OC}. Hence, there is a trade off that to increase I_{SC} by structural engineering will cause to decrease V_{OC}. At certain level, the improvement of I_{SC} can be much higher compared to the decrease of V_{OC}. Therefore, again, to obtain an optimal design, it is required to apply a comprehensive numerical calculation and analysis to obtain the optimal I_{SC}, V_{OC} and output power.

The third parameter is fill factor *FF*, which is a measure on how "square" is the output characteristic of solar cell. It is shown by the curve in the 4th quadrant of *I-V* graph in Figure-4. The shape of the curve is governed by Equation (4). It means *FF* is low for very large I_0.
The fourth parameter η, as shown in Equation (9), linearly depends on the other three parameters. Here, we can conclude that in term of structure design, increasing one of the parameter, for instance I_{SC} will cause reduction on other parameters, for example V_{OC}, and so vice versa. Finally, it is concluded that it is required to compromise between thus four output parameters to obtain the optimal condition.
When the optimalization process of four parameters from the structure given on Figure-5 is conducted by reducing the dopant concentration of one part (in general is *p*), then the solar cell will experience and have a relatively high internal resistance, which reducing output the performance parameter η. Hence, the structure in Figure-5 should be modified by inserting a layer that has a lower dopant concentration as shown in the following Figure-9, and keep the higher dopant concentration layers for ohmic contacts at the top and bottom contacts. By inserting layer *p* in between layer p^+ dan n^+ will cause the contact *p* to the contact + will have a low internal resistance, as same as between n^+ to contact -.

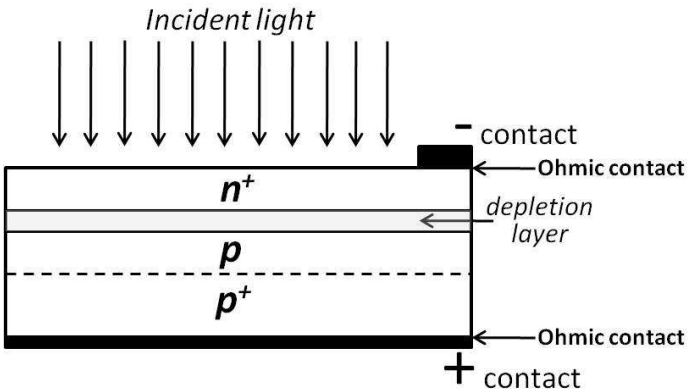

Fig. 9. Insertion of a lower dopant layer p in p-n junction diode to improve collection probability area and keep solar cell internal resistance lower.

1st generation of solar cells

1st generation of solar cell is indicated by the usage of material, which is based on silicon crystalline (c-Si). Typically solar cell is made from a single crystal silicon wafer (c-Si), with a simple p^+-p-n^+ juction diode structure (Figure-9) in large area, with bandgap energy 1.11 eV. In the development process, the usage of c-Si causes the price of solar cell very high, hence emerging the idea to use non-crystalline or poly-crystalline Si for producing solar cells. There was compromising between cost and efficiency. Using poly-crystalline material the price is cut down to the lower one since the fabrication cost is much lower, however the efficiency is going down as well, since the minority carrier lifetimes τ_e and τ_h are shorter in poly-crystalline than in single–crystalline Si that makes lower I_{photon} (Equations (3 - 5)). For the ground application with no limitation of area, it is considered to use lower price solar cells with lower conversion efficiency. However, for application with limited areas for

instances on high-rise buildings and even on satellites, space shuttles or space-lab, a higher conversion efficiency is much considered. The first generation of solar cells based on poly-crystalline Si still dominates the market nowadays. The conversion energy efficiency typically reaches 12 to 14 %.

3.2 Material engineering to improve conversion parameter *G* (electron-hole pair generation rate)

2nd generation of solar cells

Instead of based on traditional Si wafer cystalline and polycrystalline, in the 2nd Generation solar cell, it began to use material alloys such as elemental group IV alloy for instance SiGe (silicon-germanium), binary and ternary III-V group alloy for instances InGaP, GaAs and AlGaAs. Futhermore, binary to quaternary II-VI group alloy is used as well, such as Cadmium Telluride (CdTe) and Copper Indium Galium Diselenide (CIGS) alloys. The goals of using such material alloys in solar cell diode structure is to improve the irradiance photon to electric conversion rate parameter *G* such as shown in Equation (5) and has been derived in Equations (14-a and b).
By common sense, if $\lambda_{bandgap}$ is as large as possible, then we can expect that the *G* parameter goes up. This is the reason, why one applies SiGe for the solar cell, since the alloy has lower bandgap than Si, where the bandgap energy is governed by the following formula [6] where *x* represents the percent composition of Germanium:

$$E_g(x) = (1.155 - 0.43x + 0.0206x^2)eV \quad \text{for} \quad 0 < x < 0.85 \tag{17}$$

and

$$E_g(x) = (2.010 - 1.27x)eV \quad \text{for} \quad 0.85 < x < 1 \tag{18}$$

The usage of SiGe alloy for solar cell results in the improvement of conversion efficiency up to 18% [11].

Multi-junction solar cells

In the first generation, Solar cell diode structure used a single type material Si in the form of crystalline, poly-crystalline and amorphous. In the development of 2nd generation solar cell, the researchers use several material alloys in one single device, then it is called as multi-junction solar cell. As already explained and illustrated in Figure-6 that the shorter the photonic wavelength then it will be absorbed faster inside the material. It means the shorter wavelength part of the sun light spectrum will be absorbed more than the longer part of the spectrum by the same thickness of material. The wavelengths longer than the bandgap wavelength will not be absorbed at all. The part of the spectrum not absorbed by the diode material is the inefficiency of the solar cell. In order to improve solar cell efficiency performance, then the remaining unabsorbed spectrum must be reabsorbed by the next structure that can converting become electricity. The solar cell structures in the second generation are mostly in the form of tandem structure, which consists of various alloy materials that have different bandgaps with sequence from the top surface, is the highest bandgap then continued by the lower and finaly the lowest, such as illustrated on Figure-10.
There may be a question, if the lower bandgap can absorb more spectrum, why not it is used a single diode structure with very low bandgap material to absorb the overall spectrum energy? without building tandem or cascading structures. The answer is following, it is

correct that more lower the bandgap energy; the material can be categorized as more effective in photon absorption. Hence, for photons with the same wavelength will be absorb faster in lower bandgap typed material in comparison to the larger bandgap material. Thus mechanism is very clear illustrated in math relation by Equations (12 and 14a).

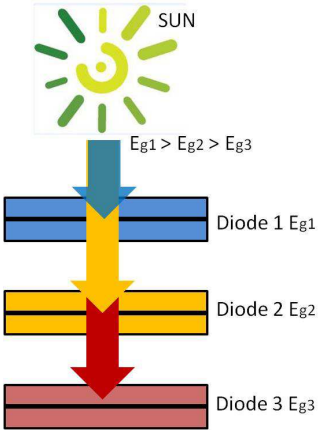

Fig. 10. Multi-junction and cell tandem concept.

The higher energy photon will be very fast absorbed and then generate hole-electron pairs with a high concentration in area close to the top surface of diode, which naturally has abundance surface defects corresponds to deep level trap close the surface. This surface defects cause a fast recombination process. Hence, it can be concluded that the usage of one diode structure with a lower bandgap energy, then a wide photon spectrum can be absorbed, however, the generated electron-hole pairs by the high energy photon will be recombined because located near the surface area with abundance defects and deep level states. Therefore, to make effective absorption and efficient conversion, the solar cell should be in the tandem structure such as illustrated in Figure-10. Further, Figure-11 shows a typical design of multi-junction or tandem solar cell incorporating III-V group of materials.
While the first generation with 12 to 14% efficiency dominates the market nowadays, this second generation of solar cells based on multi-junction structure dominates the market of high efficient solar cell as well, which typically reach 35 to 47 % efficiency. The typical applications of high efficient second generation solar cell with multi-junction technology are for satellite communications and space shuttles. To design multi-junction structure, it is required to have a knowledge about crystalline lattice match. If the crystalline lattice does not match, then there will exist abundance of deep level states in the junction region that cause a short carrier life-time or it causes faster or larger local recombination process. This large local recombination, finally will reduce the output current I_{photon}. The information regarding to the bandgap energies dan lattice match of various material are shown on Figures-12 and 13 [4] as follows.
Thus two first generations, besides of dominating solar cell technologies and markets nowadays, also are dominated by the usage of mostly silicon alloy based on semiconductor material. This situation causes the ratio of the solar cell price to the Watt-output power never decrease, because it tightly compete with the usage of Si and other semiconductor

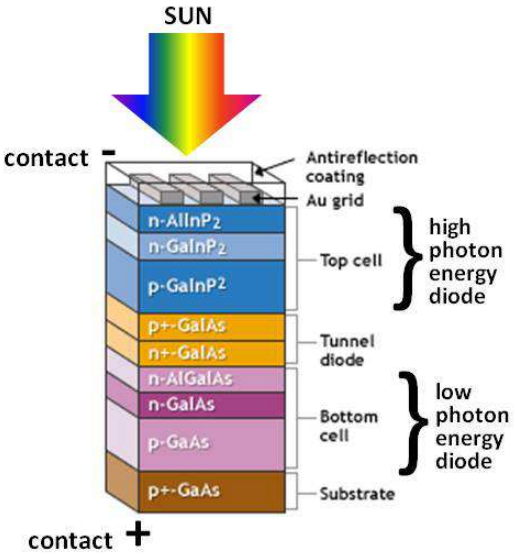

Fig. 11. Typical of high efficient solar cell with dual cell tandem structure[12].

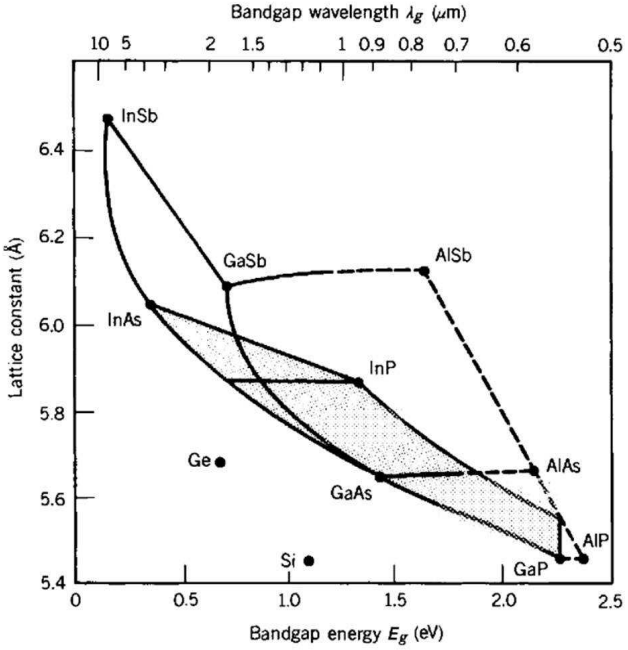

Fig. 12. Lattice constants, bandgap energies and bandgap wavelengths for III-V binary compounds, Si and Ge [4].

material for the global electronics industry demand. The condition encourages the researchers to create a radical technology revolution, by using non-crystalline material that replacing Si and other semiconductor materials, and it is realized in the form of dye-sensitized solar cell (DSSC) as the 3rd generation solar cells.

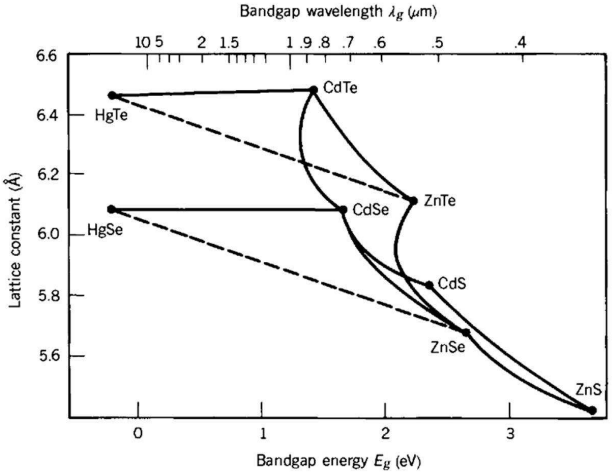

Fig. 13. Lattice constants, bandgap energies and bandgap wavelengths for important II-VI binary compounds [4].

3.3 Quantum efficiency engineering (optical design)

Antireflection (AR) thin-film coating

As already well understood that the sun-light before reaching solar cell, propagates through the vacuum and air. At the moment when the light reaches the solar cell front surface, which is made by silicon material, the light experiences of reflection by the silicon surface due to the index of refraction difference between air and silicon. The reflection causes reduction of overall efficiency of the solar cell. We have to reduce the reflection in order to increase the efficiency. By borrowing the technique that has been well developed in optical science, furthermore to reduce reflection or increase absorption, it uses antireflection thin film coating structure applied on top of the front solar cell surface. Basically this technique uses Bragg reflection phenomenon, that is an interference effect caused by thin film structure. The following Figure-14 illustrates the process of Bragg reflection occurrence by the mirror stack structure. The reflectance occurs when the light incidence on an interface of two material with different index of refraction $n_1 \neq n_2$.
The maximum reflection intensity occurs when the following condition is set and called as Bragg angle [4]

$$\sin\theta = \frac{\lambda}{2d} \tag{19}$$

For normal incidence $\theta = 90^0$, with Bragg equation, distance between mirrors needed for constructive interference reflectance is $d = \lambda/2$. While for the requirement of destructive

interference reflectance or constructive interference transmittance, the distance between mirrors is $d = \lambda/4$.

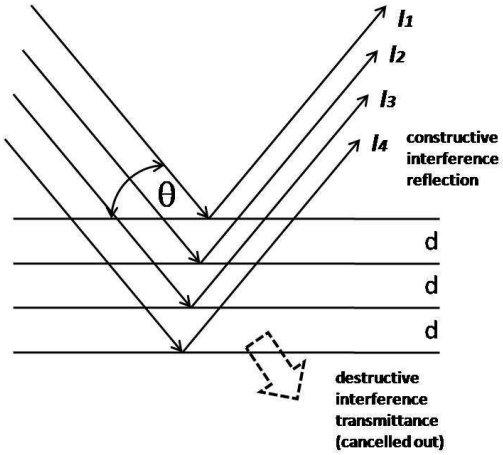

Fig. 14. Bragg reflection effect of mirror stacks structure with distance $d = \lambda/2$.

Furthermore, if there is only a single thin-film structure, as shown on Figure-15, then by using Fresnel equation and assumed that the design is for a normal incidence, then on each interface will occurs reflectance which is written as [2]

$$r_1 = \frac{n_{air} - n_{AR}}{n_{air} + n_{AR}} \quad \text{and} \quad r_2 = \frac{n_{AR} - n_{Si}}{n_{AR} + n_{Si}} \tag{20}$$

where r_1 is interface between air and antireflection coating (AR), and r_2 is interface between AR and silicon.

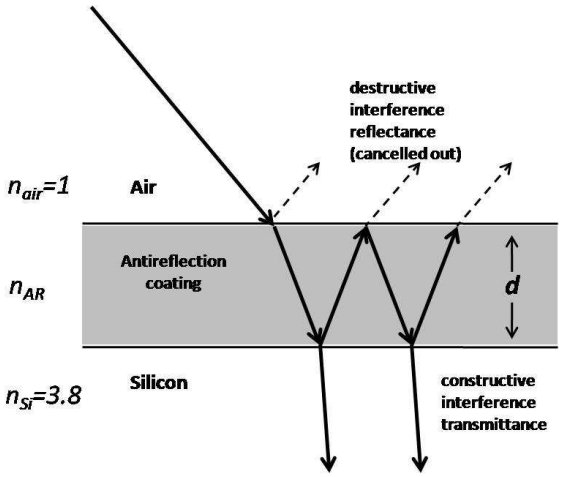

Fig. 15. Bragg reflection effect of mirror stacks structure with distance $d = \lambda/4$.

When the AR coating thickness is designed to be $n_{AR}\,d = \lambda_0 / 4$ and in normal incidence, then the total or overall reflectance is minimum and can be written as follows [2]:

$$R_{\min} = \left(\frac{n_{AR}^2 - n_{air} n_{Si}}{n_{AR}^2 + n_{air} n_{Si}} \right)^2 \tag{21}$$

Furthermore, it can be obtained zero reflectance if $n_{AR}^2 - n_{air} n_{Si} = 0$. At this condition, it means that the whole incidence sun light will be absorbed in to Si solar cell diode. As an additional information that refractive index of Si $n_{Si} \approx 3.8$ in the visible spectrum range and $n_{air} = 1$, such that to obtain $R = 0$, then required to use a dielectric AR coating with $n_{AR} \approx \sqrt{n_{air} \cdot n_{Si}} \approx 1.9$. The following Tabel-1 shows a list of materials with their corresponding refractive indices on the wavelength spectrum range in the region of visible and infrared [2].

Material	*Refractive index*
MgF_2	1.3 – 1.4
Al_2O_3	1.8 – 1.9
Si_3N_4	1.8 – 2.05
SiO_2	1.45 – 1.52
SiO	1.8 – 1.9
TiO_2	2.3
ZnS	2.3 – 2.4
Ta_2O_5	2.1 – 2.3
HfO_2	1.75 – 2.0

Tabel 1. List of Refractive Indices of Dielectric Materials

To obtain a minimum reflectance with a single thin film layer AR, we can apply Al_2O_3, Si_3N_4, SiO or HfO_2 single layer. Other material can be used as AR in multi layer thin-film structure with the consequence of higher fabrication cost.

Textured Surfaces

The other method used to reduce reflectance and at the same time increasing photon intensity absorption is by using textured surfaces [2,4]. The simple illustration, how the light can be trapped and then absorbed by solar cell diode is shown on the following Figure-16. Generally, the textured surface can be produced by etching on silicon surface by using etch process where etching silicon in one lattice direction in crystal structure is faster than etching to the other direction. The result is in the form of pyramids as shown in the following Figure-16 [2].

Beside to the one explained above, there are still many methods used to fabricate textured surface, for an example by using large area grating fabrication method on top the solar cell

structure. The large area grating fabrication is started by making photoresist grating with interferometer method, and further continued by etching to the covering layer film of top surface of solar cell structure, as has been done by Priambodo et al [7].
The pyramids shown in Figure-16 are results of intersection crystal lattice planes. Based on Miller indices, the silicon surface is aligned parallel to the (100) plane and the pyramids are formed by the (111) planes [2].

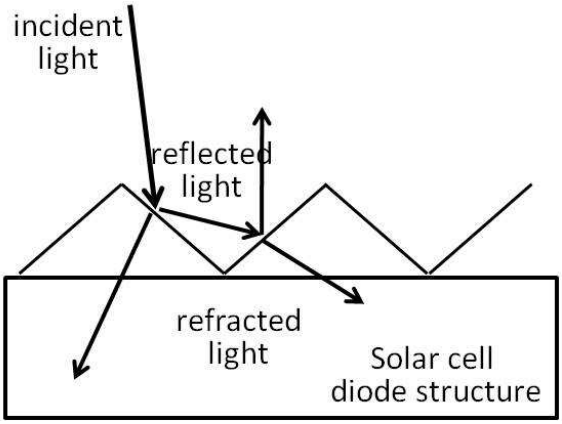

Fig. 16. Textured surface solar cell to improve absorption of solar photons.

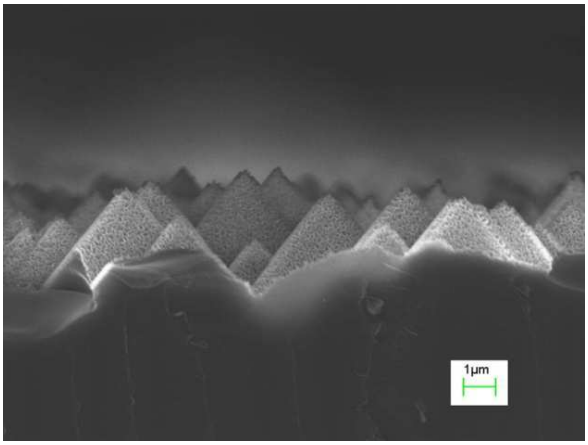

Fig. 17. The Appearance of a textured silicon surface under an SEM [2].

In order to obtain more effective in trapping sun-light to be absorbed, the textured surface design should consider the diffraction effects of textured surface. The diffraction or grating equation is simply written as the following [4]:

$$\sin\theta_q = \sin\theta_i + q\frac{\lambda}{\Lambda} \tag{22}$$

where θ_i is the incidence angle to the normal of the grating surface and θ_q is diffracted order angle, Λ is grating period and λ is photonic wavelength. When θ_i is set = 0 or incidence angle normal to the grating and $\Lambda < \lambda$, then the diffracted order photon close 90^0 or becoming surface wave on the surface of the solar cell structure. Because the refractive index of Si solar cell diode higher than the average textured surface, and if the thickness of textured surface $d_{ts} < \lambda/4n_{Si}$, then it can be concluded that the whole incident photon energy will be absorbed in to solar cell diode device.

Priambodo et al [7] in their paper shows in detail to create and fabricate textured surface for guided mode resonance (GMR) filter by using interferometric pattern method. We can assume the substrate is solar cell diode structure, which is covered by thin film structure hafnium dioxide (HfO_2) and silicon dioxide (SiO_2). The first step is covering the thin film structure on solar cell by photoresist by using spin-coater, then continued by exposing to a large interferometric UV and developed such that result in large area photoresist grating with period < 400 nm as shown in SEM picture of Figure-18, as follows.

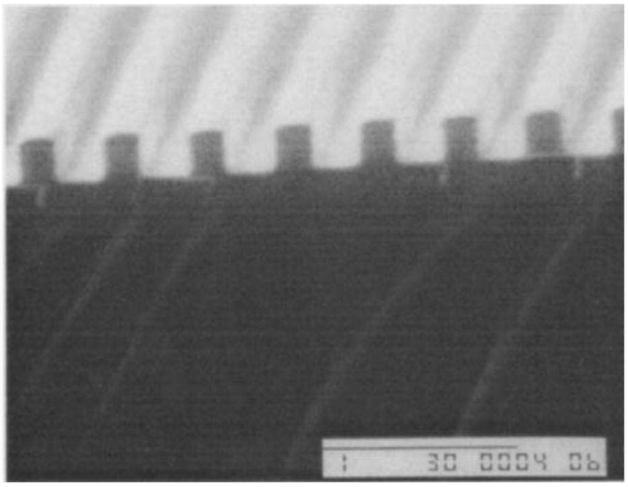

Fig. 18. SEM Picture of grating pattern on large surface with submicron period. This zero order diffracting layer is perfect to be applied for antireflection large area solar cell [7].

Furthermore, on top of the photoresist grating pattern, it is deposited a very thin layer of chromium (Cr) ~ 40-nm by using e-beam evaporator. The next step is removing the photoresist part by using acetone in ultrasonic washer, and left metal Cr grating pattern as a etching mask on top of thin film structure. Moreover, dry etching is conducted to create a large grating pattern on the thin film SiO_2/HfO_2 structure on top of solar cell, by using reactive ion etch (RIE). The whole structure of the solar cell device is shown on Figure-19 below.

However, even though having advantages in improvement of gathering sun-light, but the textured surface has several disadvantages as well, i.e.: (1) more care required in handling; (2) the corrugated surface is more effective to absorb the photon energy in wide spectrum that may some part of it not useful to generate electric energy and causing heat of the solar cell system [2].

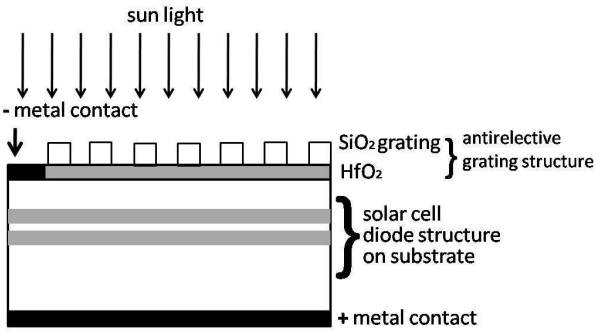

Fig. 19. Solar cell structure incorporating antireflective grating structure.

Top-contact design

For solar cell, which is designed to have a large current delivery capacity, the top-contact is a part of solar cell that must be considered. For large current delivery, it is required to have a large top-contact but not blocking the sunlight comes in to the solar cell structure. The design of top-contact must consider that the current transportation is evenly distributed, such that prohibited that a large lateral current flow in top surface. The losses occur in solar cell, mostly due to top-surface lateral current flow and the bad quality of metal contact with semiconductor as well, hence creates a large high internal resistance. For those reasons, the top contact is designed to have a good quality of metal semiconductor contact in the form of wire-mesh with busbars, which are collecting current from the smaller finger-mesh, as shown on Figure-20 [2]. The busbars and the fingers ensure suppressing the lateral current flow on the top surface.

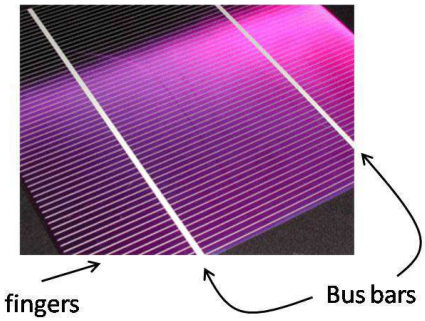

Fig. 20. An Example of top-contact design for solar cells [2].

Concentrating system engineering

The solar cell system efficiency without concentrating treatment, in general, is determined by ratio converted electrical energy to the light energy input, which corresponds to total the lumen of sun irradiance per unit area m^2. This is a physical efficiency evaluation. In general, the solar cells available in the market have the efficiency value in the range of 12 – 14%. This efficiency value has a direct relationship to the cost efficiency, which is represented in ratio Wattage output to the solar cell area in m^2. Device structure and material engineering

discussed in the previous section, are the efforts to improve conversion efficiency in physical meaning. However, the concentrating system engineering we discussed here is an effort to improve the efficiency ratio output wattage to the cost only. In the physics sense, by the concentrating system, the solar cell device efficiency is not experiencing improvement, however in cost efficiency sense, it is improved.

The general method used for concentrating system engineering is the usage of positive (convex) lens to gather the sun irradiance and focus them to the solar cell. By concentrating the input lumen, it is expected there will be an improvement of output electricity. If the lens cost is much lower compared to the solar cell, then it can be concluded that overall it is experiencing improvement in cost efficiency. Another method for concentrating system engineering is the usage of parabolic reflector to focus sun irradiance which is collected by large area of parabolic reflector then focused to the smaller solar cell area. Both examples concentrating system engineering are shown on Figure-21 [2].

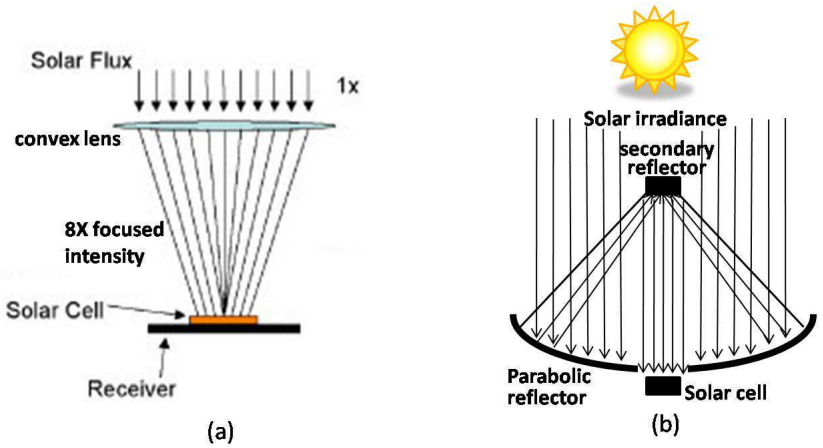

Fig. 21. Two examples of concentrating system engineering concepts with (a) convex lens and (b) parabolic reflector [2].

The technical disadvantages of applying concentrator on solar cell is that the solar cell must be in normal direction to the sun, having larger area and heavier. This means that the system require a control system to point to the sun and finally caused getting more expensive. The cost efficiency should consider thus overall cost.

4. Standard solar cell fabrications

Since the first time developed in 1950s, solar cells had been applied for various applications, such as for residential, national energy resources, even for spacecrafts and satellites. To make it systematic, as available in the market today, we classify the solar cell technologies in 3 mainstreams or generations. The first generation is based on Si material, while the second generations are based on material alloys of group IV, III-V and II-VI, as already explained in Section-3. While the third generation is based on organic polymer, in order to reduce the cost, improve Wattage to cost ratio and develop as many as possible solar cell, such as developed by Gratzel et al [10]. In this section, we will discuss the standard fabrication

available for solar cell fabrication for the first and second generations, by using semiconductor materials and the alloys.

Standard Fab for 1st generation

Up to now, the market is still dominated by solar cell based on Si material. The reason why market still using Si is because the technology is settled down and Si wafer are abundance available in the market. At the beginning, the solar cells used pure crystalline Si wafers, such that the price was relatively high, because the usage competed with electronics circuit industries. Moreover, there was a trend to use substrate poly crystalline Si with lower price but the consequence of energy conversion efficiency becoming lower. The energy-conversion efficiency of commercial solar cells typically lies in between 12 to 14 % [2].

In this section, we will not discuss how to fabricate silicon substrate, but more emphasizing on how we fabricate solar cell structure on top of the available substrates. There are several mandatory steps that must be conducted prior to fabricate the diode structure.

1. Cleaning up the substrate in the clean room, to ensure that the wafer free from the dust and all contaminant particles attached on the wafers, conformed with the standard electronic industries, i.e. rinsing detergent (if needed), DI water, alcohol, acetone, TCE dan applying ultrasonic rinsing.
2. After cleaning step, it is ready to be continued with steps of fabricating diode structure on wafer.

There are several technologies available to be used to fabricate solar cell diode structure on Si wafer. In this discussion, 2 major methods are explained, i.e.: (1) chemical vapor diffusion dan (2) molecular beam epitaxy (MBE).

In Si semiconductor technology, it is common to make p-type Si wafer needs boron dopant to be the dopant acceptor in Si wafer, i.e. the material in group III, which is normally added to the melt in the Czochralski process. Furthermore, in order to make n-type Si wafer needs phosporus dopant to be the dopant donor in Si wafer, i.e. the material in group V. In the solar cell diode structure fabrication process in the 1st generation as shown in Figure-9, it is needed a preparation of p-type Si wafer, in this case a high concentration p or p^+. Moreover, we have to deposit 2 thin layers, p and n^+ respectively on top of the p+ wafer. In order make the p^+pn^+ diode structure, we discuss one of the method, which is very robust, i.e. by using chemical vapor diffusion method, such as shown in the following Figure-22 [2].

Instead of depositing layers p and n^+ on top of p^+ substrate, in this process phophorus dopants are diffused on the top surface of p^+ substrate. As already known, phosphorus is a common impurity used. In this common process, a carrier gas (N_2) is drifted into the $POCl_3$ liquid creates bubles mixed of $POCl_3$ and N_2, then mixed with a small amount of oxygen, the mixed gas passed down into the heated furnace tube with p-type of Si wafers stacked inside. At the temperature about 800^0 to 900^0 C, the process grows oxide on top of the wafer surface containing phosphorus, then the phosphorus diffuse from the oxide into the p-type wafer. In about 15 to 30 minutes the phosphorus impurities override the boron dopant in the region about the wafer surface, to set a thin-film of heavily doped n-type region as shown in Figure-9. Naturally, phosphorus dopant is assumed to be diffused into p^+ type substrate with an exponential function distribution

$$N_d(z) = c_0 e^{-z} \tag{22}$$

Hypothetically $c_0 = |n^+| + |p^+|$, hence, there will be a natural structure of p^+pinn^+ instead of expected p^+pn^+. The diffusion depth and c_0 are mostly determined by the concentration of

$POCl_3$ and the temperature of furnace. The distribution $N_d(z)$ dapat diatur sehingga the thickness of pin layer between p^+ and n^+ can be made as thin as possible, such that can be ignored. In the subsequent process, after pulled out the wafers from the furnace, the oxide layer is removed by using HF acid.

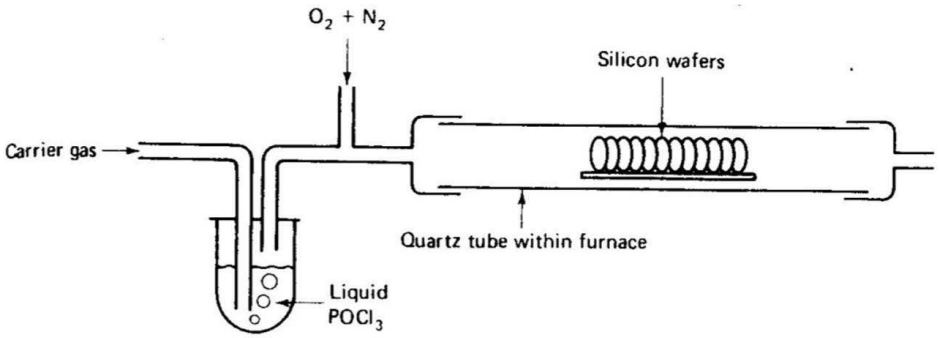

Fig. 22. Chemical (phosphorus) diffusion process [2].

Metal contacts for both top and bottom contacts are applied by using a standard and conventional technology, well known as vacuum metal evaporation. The bottom metal contact of p^+ part can be in the form of solid contact; however, the top contact should be in the form of wire-mesh with bus-bars and fingers as explained in previous section. To develop such wire-mesh metal contact for top surface, it is started with depositing photo-resist on the top surface by spin-coating, continued by exposed by UV system, incorporating wire-mesh mask and finally developing the inverse photo-resist wire-mesh pattern. The further step is depositing metal contact layer by using a vacuum metal evaporator, which then continued by cleaning up the photo-resist and unused metal deposition by using acetone in the ultrasonic cleaner. Furthermore, to obtain a high output voltage of solar cell panel, it is required to set a series of several cells.

Standard Fab for 2nd generation

The fabrication technology that introduced in the first generation seems to be very simple, however, this technology promises very effective and cost and time efficient for mass or large volume of solar cell production. On the other side, the limited applications such as for spacecrafts and satellites require higher efficiency solar cell, with much higher prices. Every single design should be made as precise and accurate as possible. A high efficient solar cell must be based on single crystalline materials.

For that purposes, it is required an apparatus that can grow crystalline structures. There are several types of technologies the their variances, which are available to grow crystalline structures, i.e. molecular beam epitaxy (MBE) dan chemical vapor deposition (CVD).

Because of limited space of this chapter, CVD is not explained, due to its similarity principles with chemical vapor diffusion process, explained above. Furthermore, MBE is one of several methods to grow crystalline layer structures . It was invented in the late 1960s at Bell Telephone Laboratories by J. R. Arthur and Alfred Y. Cho [8]. For MBE to work, it needs an ultra vacuum chamber condition (super vacuum at 10^{-7} to 10^{-9} Pa), such that it makes possible the material growth epitaxially on crystalline wafer. The disadvantage of this MBE process is the slow growth rate, typically less than 1000-nm/hour.

Due to the limitation space of this Chapter, CVD will not be discussed, since it has similar principal work with chemical vapor difussion process. Furthermore, MBE is one of several methods to grow crystalline layer structures . It was invented in the late 1960s at Bell Telephone Laboratories by J. R. Arthur and Alfred Y. Cho.[1] In order to work, it requires a very high vacuum condition (super vacuum 10^{-7} to 10^{-9} Pa), Such that it is possible to grow material layer in the form of epitaxial crystalline. The disadvantage of MBE process is its very low growth rate, that is typically less than 1000-nm/hour. The following Figure-23 shows the detail of MBE.

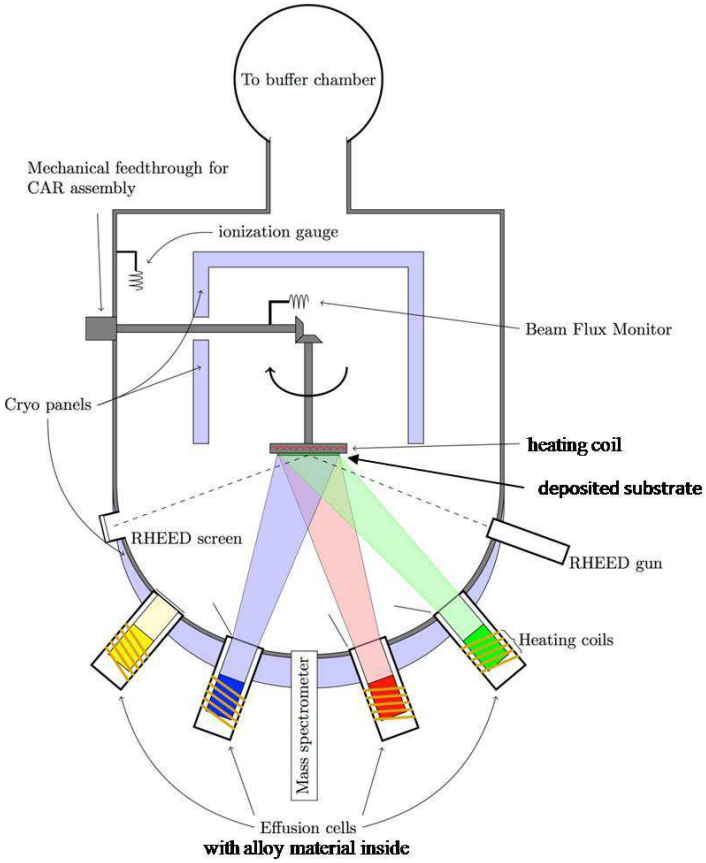

Fig. 23. Molecular beam epitaxy components [8].

In order that the growing thin film layer can be done by epitaxial crystalline, the main requirements to be fulfilled are: (1) Super vacuum, such that it is possible for gaseous alloy material to align their self to form epitaxial crystalline layer. In super vacuum condition, it is possible for heated alloy materials for examples: Al, Ga, As, In, P, Sb and etc can sublimate directly from solid to the gaseous state with relatively lower temperature; (2) Heated alloy materials and the deposited substrate that makes possible the occurrence crystalline condensation form of alloy materials on the substrate; (3) Controlled system temperature,

which makes possible of controlling alloy material and substrate temperatures accurately. Typically, material such as As needs heating up to 250^0C, Ga is about 600^0C and other material requires higher temperature. In order to stable the temperature, cooling system like cryogenic system is required; and (4) Shutter system, which is used to halt the deposition process.

For example, alloy material layer such as $Al_xGa_{1-x}As$ growth on GaAs. Controlling the value of x can be conducted by controlling the temperatures of both material alloy sources. The Higher the material temperature means the higher gaseous material concentration in the chamber. More over, the higher material alloy concentration in the chamber, it will cause the higher growth rate of the alloy layer. For that reasons, the data relating to the growth rate of crystalline layer vs temperature, must be tabulated to obtain the accurate and precise device structure.

MBE system is very expensive, because the product output is very low. However, the advantage of using MBE system is accuracy and precision structure, hence resulting in relatively high efficiency and fit to be applied for production of high efficiency solar cells for satellites and spacecrafts.

5. Dye Sensitized Solar Cell (DSSC)

3rd generation of solar cell

Dye-Sensitized Solar Sel (DSSC) was developed based on the needs of inexpensive solar cells. This type is considered as the third generation of solar cell. DSSC at the first time was developed by Professor Michael Gratzel in 1991. Since then, it has been one of the topical researches conducted very intensive by researchers worldwide. DSSC is considered as first break through in solar cell technology since Si solar cell. A bit difference to the conventional one, DSSC is a photoelectrochemical solar cell, which use electrolyte material as the medium of the charge transport. Beside of electrolyte, DSSC also includes several other parts such nano-crystalline porous TiO_2, dye molecules that absorbed in the TiO_2 porous layer, and the conductive transparence ITO glass (indium tin oxide) or TCO glass (transparent conductive oxide of SnO_2) for both side of DSSC. Basically, there are 4 primary parts to build the DSSC system. The detail of the DSSC components is shown in the following Figure-24 [9-10].

The sun light is coming on the cathode contact side of the DSSC, where TCO is attached with TiO_2 porous layer. The porous layer is filled out by the dye light absorbent material. This TiO_2 porous layer with the filling dye act as *n*-part of the solar cell diode, where the electrolyte acts as *p*-part of the solar cell diode. On the other side of DSSC, there is a platinum (Pt) or gold (Au) counter-electrode to ensure a good electric contact between electrolytes and the anode. Usually the counter-electrode is covered by catalyst to speed up the redox reaction with the catalyst. The redox pairs that usually used is I^-/I_3^- (iodide/triiodide).

The Dye types can be various. For example we can use Ruthenium complex. However, the price is very high, we can replace it with anthocyanin dye. This material can be obtained from the trees such as blueberry and etc. Different dyes will have different sensitivity to absorb the light, or in term of conventional solar cell, they have different *G* parameter. The peak intensity of the sun light is at yellow wavelength, which is exactly that many dye absorbants have the absorbing sensitivity at the yellow wavelength.

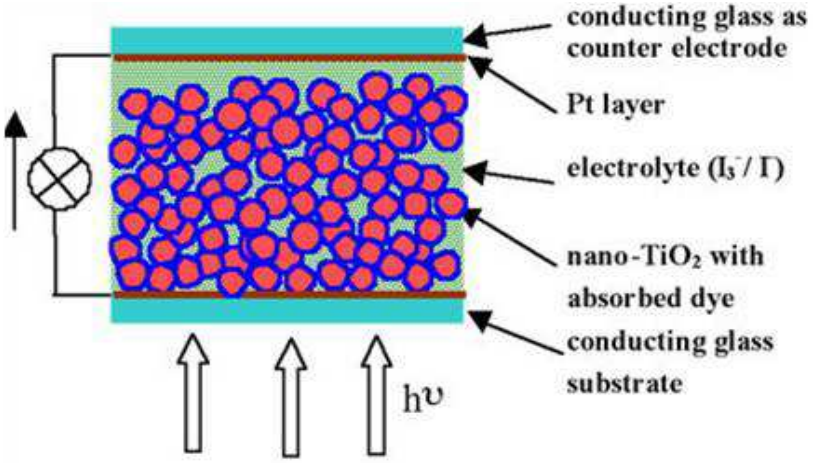

Fig. 24. The schematic diagram of DSSC.

The principal work of DSSC

The principle work of DSSC is shown in the following Figure-25. Basically the working principle of DSSC is based on electron excitation of dye material by the photon. The starting process begins with absorption of photon by the dyes, the electron is excited from the groundstate (D) to the excited state (D*). The electron of the excited state then directly injected towards the conduction band (ECB) TiO_2, and then goes to the external load, such that the dye molecule becomes more positive (D+). The lower electron energy flow from external circuit goes back to the counter-electrode through the catalyst and the electrolyte then supplies electron back to the dye D+ state to be back to the groundstate (D). The *G* parameter of DSSC depends mainly on the dye material and the thickness of TiO2 layer also the level of porosity of the TiO2 layer.

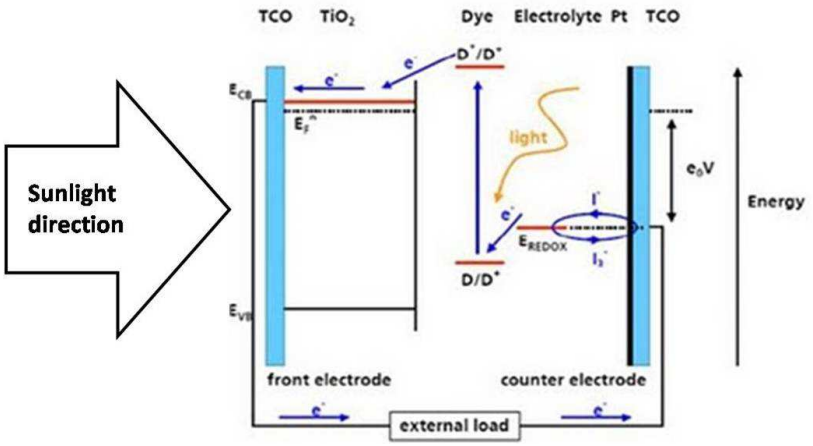

Fig. 25. The principles work of DSSC.

6. Summary

The solar cell design has been evolving in many generations. The first generation involved Si material in the form single crystalline, poly-crystalline and amorphous. There is a trade-off in the usage of single crystalline, polycrystalline or amorphous. Using single crystalline can be expected higher efficiency but higher cost than the polycrystalline solar cell. To obtain optimal design, the Chapter also discuss to get the optimal 4 output parameters, I_{SC} , V_{OC} , FF and η. Moreover, to improve the efficiency, some applying anti-relection coating thin film or corrugated thin film on top of solar cell structure. The second generation emphasize to increase the efficiency by introducing more sophisticated structure such as multi-hetero-junction structure which has a consecuence of increasing the cost. Hence there is a tradeoff in designing solar cell, to increase the conversion efficiency will have a consecuence to lower the cost efficiency or vice verca. Hence, there must be an optimal values for both conversion energy and cost efficiencies.

There is a breaktrough technology that radically changes our dependency to semiconductor in fabricating solar cell, i.e by using organic material. It is called as dye sensitized solar cell (DSSC). This technology, so far still produce lower efficiency. However, this technology is promising to produce solar cell with very low cost and easier to produce.

7. References

[1] R.F. Pierret, “Semiconductor Device Fundamentals,” Addison-Wesley Publishing Company, ISBN 0-201-54393-1, 1996

[2] M.A. Green, “Solar Cells, Operating Principles, Technology and System Applications,” Prentice Hall, ISBN 0-13-82270, 1982

[3] T. Markvart and L. Castaner, “Solar Cells, materials, Manufacture and Operation,” Elsevier, ISBN-13: 978-1-85617-457-1, ISBN-10: 1-85617-457-3, 2005

[4] B.E.A. Saleh and M.C. Teich, “Fundamentals of Photonics,” Wiley InterScience, ISBN 0-471-83965-5

[5] http://pvcdrom.pveducation.org/CELLOPER/COLPROB.HTM

[6] B.S. Meyerson, "Hi Speed Silicon Germanium Electronics". *Scientific American, March 1994, vol. 270.iii pp. 42-47.*

[7] P.S. Priambodo, T.A. Maldonado and R. Magnusson, “ Fabrication and characterization of high quality waveguide-mode resonant optical filters,” Applied Physics Letters, Vol. 83 No 16, pp: 3248-3250, 20 Oct 2003

[8] Cho, A. Y.; Arthur, J. R.; Jr (1975). ""Molecular beam epitaxy"". Prog. Solid State Chem. 10: 157–192

[9] J. Poortmans and V. Arkhipov, “ Thin film solar cells, fabrications, characterization and applications,” John Wiley & Sons, ISBN-13: 078-0-470-09126-5, 2006

[10] M. Grätzel, J. Photochem. Photobiol. C: Photochem. Rev. 4, 145–153 (2003)

[11] Usami, N. ; Takahashi, T. ; Fujiwara, K. ; Ujihara, T. ; Sazaki, G. ; Murakami, Y.; Nakajima, K. “Si/multicrystalline-SiGe heterostructure as a candidate for solar cells with high conversion efficiency”, Photovoltaic Specialists Conference, 2002. Conference Record of the Twenty-Ninth IEEE, 19-24 May 2002

[12] Andreev, V.M.; Karlina, L.B.; Kazantsev, A.B.; Khvostikov, V.P.; Rumyantsev, V.D.; Sorokina, S.V.; Shvarts, M.Z.; "Concentrator tandem solar cells based on AlGaAs/GaAs-InP/InGaAs(or GaSb) structures", Photovoltaic Energy Conversion, 1994., Conference Record of the Twenty Fourth. IEEE Photovoltaic Specialists Conference - 1994, 1994 IEEE First World Conference on, 5-9 Dec 1994

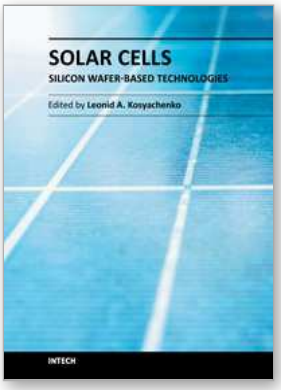

Solar Cells - Silicon Wafer-Based Technologies

Edited by Prof. Leonid A. Kosyachenko

ISBN 978-953-307-747-5
Hard cover, 364 pages
Publisher InTech
Published online 02, November, 2011
Published in print edition November, 2011

The third book of four-volume edition of 'Solar Cells' is devoted to solar cells based on silicon wafers, i.e., the main material used in today's photovoltaics. The volume includes the chapters that present new results of research aimed to improve efficiency, to reduce consumption of materials and to lower cost of wafer-based silicon solar cells as well as new methods of research and testing of the devices. Light trapping design in c-Si and mc-Si solar cells, solar-energy conversion as a function of the geometric-concentration factor, design criteria for spacecraft solar arrays are considered in several chapters. A system for the micrometric characterization of solar cells, for identifying the electrical parameters of PV solar generators, a new model for extracting the physical parameters of solar cells, LBIC method for characterization of solar cells, non-idealities in the I-V characteristic of the PV generators are discussed in other chapters of the volume.

InTech Europe
University Campus STeP Ri
Slavka Krautzeka 83/A
51000 Rijeka, Croatia
Phone: +385 (51) 770 447
Fax: +385 (51) 686 166
www.intechopen.com

InTech China
Unit 405, Office Block, Hotel Equatorial Shanghai
No.65, Yan An Road (West), Shanghai, 200040, China
中国上海市延安西路65号上海国际贵都大饭店办公楼405单元
Phone: +86-21-62489820
Fax: +86-21-62489821